

# Vibratory Fruit Harvesting: A Linear Theory of Fruit-stem Dynamics

J. R. COOKE\* ; R. H. RAND†

A linearized, three-degree-of-freedom model of a fruit-stem system which is excited by simultaneous, periodic horizontal and vertical planar displacements (any straight line, ellipse, or circle) of the supporting structure was examined in relation to vibratory fruit harvesting. The regions of dynamic instability and the corresponding modal shapes were inferred from the coupled, nonhomogeneous Hill's equations which describe the motion of the double physical pendulum with torsion springs. The frequency conditions for fruit separation or detachment with or without the stem attached to the fruit may be predicted. Although the model is generally applicable to all freely, vertically suspended fruits, special consideration was given to apples. The surface area, volume, and moments of inertia for the apple, orange, and lemon-shaped geometries of a bispherical coordinate system were analytically determined. References to the available data on the relevant physical properties of fruits and stems were given.

## 1. Introduction

The mechanization of fruit harvesting has been a major goal of the agricultural engineering profession for nearly a decade. Apples, peaches, pears, plums, prunes, apricots, grapes, lemons, grapefruit, cherries, olives and coffee may now be mechanically harvested; the inertial type shakers have been especially successful in harvesting the processing fruit.

The development of these successful machines has been mainly of an empirical nature. This paper describes a mathematical analysis of the major aspects of the dynamic behaviour of the fruit and stem during simultaneous horizontal and vertical forcing of the fruit support structure. Hopefully, the mathematical model to be formulated is sufficiently general so as to unify much of the experimental work, to identify the need for certain important data which are not currently available, and to make certain useful predictions.

Can the stroke direction and frequency be adjusted so as to cause efficient fruit detachment, with or without stems, as desired?<sup>1-3</sup> Historically, much emphasis has been given to the conditions required for displacement resonance of the tree structure<sup>4</sup> rather than the fruit-stem combination. Separation, it was reasoned, would occur when a maximum tensile stem force was produced by vigorous shaking. The quasi-static force required for fruit removal is known to depend upon the angle of application of the force with respect to the fruit's natural orientation,<sup>2, 5, 6</sup> stage of maturity, and environmental history. The tensile stem force to weight ratio, however, appears to be a poor indicator of the optimal harvesting parameters.<sup>5, 7, 8</sup> Rather, the importance of fatigue failure of the stem during repeated bending is important.<sup>7, 8, 10</sup> The number of cycles required to produce stem failure has been investigated for apples,<sup>6, 11-13</sup> for olives,<sup>7</sup> for lemons,<sup>2</sup> and for coffee.<sup>9</sup> Diener,<sup>15</sup> for example, reported an average shaking time for Jonathan apples of 4.1 s with 85% removal in 25 strokes. Moore *et al.*<sup>6</sup> have studied in greater detail two other apple varieties at frequencies from 120 to 600 cycles per minute with various amplitudes.

Analyses for fruit-stem behaviour due to vibration have been developed for grapes,<sup>10, 14</sup> coffee,<sup>8</sup> apples,<sup>12, 15</sup> cherries and olives,<sup>16</sup> and oranges and grapefruit.<sup>17</sup> Three analyses<sup>18, 8, 17</sup> have considered the problem as a transverse vibration of a cantilever beam with a tip mass.

In one instance,<sup>18</sup> the tensile attachment force of a fruit directly attached to a member undergoing harmonic vertical oscillations was examined. As shown by more recent studies, the separation rarely occurs in this fashion.<sup>2, 7</sup> Another researcher<sup>8</sup> indicated, but did not solve, the problem

\*Assistant Professor of Agricultural Engineering, Cornell University, Ithaca

†Assistant Professor of Theoretical and Applied Mechanics, Cornell University, Ithaca

as a cantilever with tip mass. More recently, Rumsey applied the classical Bernoulli-Euler beam theory to a vertical stem with fruit attached. The rotary inertia of the attached fruit mass was neglected. The significance of this assumption<sup>19, 20</sup> may be great since the mass of the stem is less than one per cent of the fruit-stem system mass.

The earliest analysis of the fruit-stem system<sup>10, 14</sup> was based upon a freely hinged, one degree-of-freedom, physical pendulum. The instabilities of the linearized system due to (non-simultaneous) horizontal or vertical harmonic forcings were discussed. The observed behaviour of apples<sup>15</sup> includes five modes of oscillation, three of which are especially important in harvesting (see *Fig. 1*). In the pendulum mode, the fruit and stem oscillate in phase and pivot about the abscission layer. In the tilting mode, the stem and fruit are out of phase and pivot at the fruit-stem junction. The third mode results in rotation of the fruit about an axis which coincides with the stem. Similar observations for oranges and grapefruits have been made by Rumsey.<sup>17</sup> Thomas<sup>12</sup> has extended the generality of the pendulum analysis to include a spring constant and damping in the one degree-of-freedom model.

More recently, Studer has experimentally applied the one degree-of-freedom model to olives and cherries with good agreement, but has expressed concern that some fruit would be scattered and damaged during the instability.

## 2. Analysis

It is desirable to know the optimal frequency or range of frequencies for vibratory fruit removal. We propose to calculate such frequencies on the basis of a mathematical model of a fruit, including its stem. The tree limb is ignored in the analysis; and hence, we assume that the damping and arrangement of the limb structure is such that the effective driving frequency of the vibrator is not appreciably altered by the limbs as the effect of the vibrator is transmitted through the limbs to the fruit.<sup>15</sup>

Although the physical situation of vibratory fruit removal involves large deflections of the fruit, the associated mathematics becomes nonlinear when large deflections are entertained and, hence, difficult to solve. It will be eventually of interest to study the large deflection problem, but here we will treat the small deflection problem with the following explanation. In order for the deflections to build up to large values from rest, it is necessary that they first take on small values. If it is found in the small deflection analysis that certain motions remain small for all time (i.e. are stable), then these will never build up to large deflections and the fruit will not be removed due to a vibration at a frequency causing these motions. (It is assumed that the fruit is removed due to the stresses caused by large deflections of the fruit relative to the stem or the stem relative to the support.) Similarly, if it is found that certain motions are unbounded in the linear analysis as time gets very large (i.e. are unstable), then these will in general lead to large deflections and fruit removal. The faster the unstable motion blows up, the faster, we say, the fruit will be removed. Therefore, the optimal driving frequency in the linear analysis will correspond to the most unstable solution.

It is further assumed that the damping in the fruit stem is small enough so that the resonant frequencies of an undamped model do not differ greatly from the resonant frequencies of the same model with damping. (It is well known that for a damped harmonic oscillator with small damping, the resonant frequency is nearly equal to the resonant frequency of the same oscillator without damping.) The damping in apples has been examined by Thomas.<sup>12</sup>

Although the original motion of the vibrator may be purely vertical or purely horizontal, the motion of the support of the fruit-stem model will generally exhibit both vertical and horizontal components because of the flexibility of the limb structure. It is, therefore, desirable to drive the support of the fruit-stem model in a direction which is neither purely vertical nor purely horizontal but rather partly both. The simplest Lissajous figures<sup>21</sup> will be of interest. In particular, if the horizontal and vertical forcing frequencies are the same, the amplitudes and phase angles may be

adjusted to describe elliptic paths of arbitrary orientation. Circular and straight line paths are special cases of elliptic motion.

It is desirable that the choice of the fruit-stem model exhibit the three degrees of freedom experimentally observed for apples<sup>15</sup> (Fig. 1). These may be described as an in-phase planar motion, an out-of-phase planar motion, and a twisting motion. Although the plane of the planar model will in general be undetermined *a priori*, in the model chosen for study the plane of motion is fixed at once. Thus, the model is thought to be the simplest system possessing the geometry and dynamics exhibited by the physical problem. Extensions of this work to more complicated models are, of course, desirable and would include effects of friction, nonlinearity, and nonfixed plane of motion.

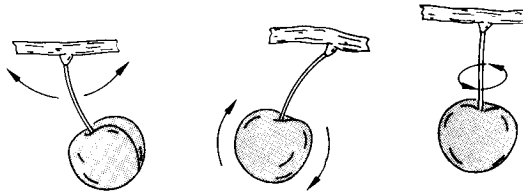


Fig. 1. The three important modes of oscillation for apples as described by Diener (Left) pendulum mode; (Centre) tilting mode; (Right) twisting mode

The model chosen for this analysis is shown in Fig. 2. It consists of a double compound pendulum with torsion springs. The upper torsion spring of spring constant  $S$  represents the lumped flexibility of the stem; the stem is represented by a thin, rigid rod of mass  $\mu$  and length  $L$ . The lower torsion springs represent the lumped flexibility of the fruit-stem socket and have spring constant  $K$  for the in-plane motion and spring constant  $C$  for the twisting motion. The fruit is represented by a sphere of mass  $M$  and radius  $R$ . The three generalized co-ordinates are chosen to be:  $\theta$ , the angle of deflection of the rod from the vertical;  $\phi$ , the angle of deflection of the sphere from the vertical; and  $\psi$ , the angle of twist of the sphere.

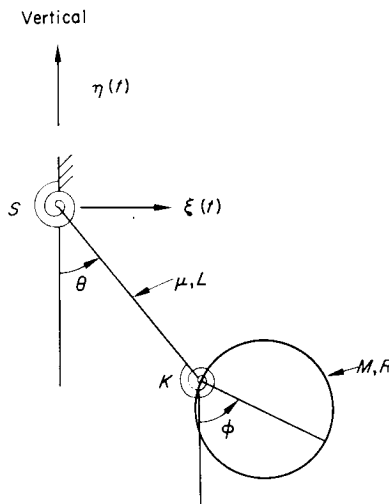


Fig. 2. Mathematical model of a fruit with stem subject to periodic, elliptic excitation. Not shown is the torsion spring with spring constant  $C$  which resists the twisting displacement  $\psi$  of the sphere relative to the rod

It is of interest to find the natural frequencies of this model. The potential energy is found to be:

$$V=(1/2)S\theta^2+(1/2)K(\varphi-\theta)^2+(1/2)C\psi^2-\mu g(L/2)\cos\theta-Mg(L\cos\theta+R\cos\varphi).$$

The kinetic energy may be written:

$$T=(1/6)\mu L^2 \dot{\theta}^2+(1/2)M [L^2 \dot{\theta}^2+R^2 \dot{\varphi}^2+2RL\dot{\theta}\dot{\varphi}\cos(\theta-\varphi)]+(1/5)MR^2 (\dot{\varphi}^2+\dot{\psi}^2).$$

Using these expressions, Lagrange's equations for the co-ordinates  $\theta$ ,  $\varphi$ , and  $\psi$  respectively become, upon neglecting nonlinear terms:

$$\begin{aligned} [(\mu/3)+M] L^2\ddot{\theta}+MLR\dot{\varphi}+S\theta+K(\theta-\varphi)+[(\mu/2)+M] gL\theta &=0 \\ (7/5)MR^2\ddot{\varphi}+MLR \ddot{\theta}+K(\varphi-\theta)+MgR\varphi &=0 \\ (2/5)MR^2\ddot{\psi}+C\psi &=0 \end{aligned}$$

For free vibrations, set:

$$\begin{aligned} \theta &=\bar{\theta} \exp(i\omega t) \\ \varphi &=\bar{\varphi} \exp(i\omega t) \\ \psi &=\bar{\psi} \exp(i\omega t) \end{aligned}$$

where  $\bar{\theta}$ ,  $\bar{\varphi}$ , and  $\bar{\psi}$  are constants and where  $\omega$  is the natural frequency. Substituting these into the linearized equations of motion, it is clear that there is an uncoupling between the twisting motion and the planar motions. For the twisting mode:

$$\omega^2 = \frac{5C}{2MR^2}$$

while for the planar modes, the natural frequencies are the roots of the equation:

$$(a_1+a_2\omega^2)^2-(a_3\omega^2-a_4)(a_5\omega^2-a_6)=0 \tag{1}$$

where

$$\begin{aligned} a_1 &=K \\ a_2 &=MRL \\ a_3 &=[(\mu/3)+M]L^2 \\ a_4 &=S+K+[(\mu/2)+M] gL \\ a_5 &=(7/5)MR^2 \\ a_6 &=MgR+K. \end{aligned}$$

The mode shapes for the planar modes may be found from:

$$(\bar{\varphi}/\bar{\theta})=[K+MLR\omega^2]/[-(7/5)MR^2\omega^2+MgR+K]. \tag{2}$$

Now suppose the support of the model is given a horizontal motion  $\xi(t)$  and a vertical motion  $\eta(t)$  (see Fig. 2). Then, Lagrange's equation for the co-ordinate  $\psi$  is unchanged, but the linearized equation for  $\varphi$  and  $\theta$  becomes

$$A\ddot{x}+Bx=v$$

where

$$\begin{aligned} x &= \begin{bmatrix} \theta \\ \varphi \end{bmatrix} \\ A &= \begin{bmatrix} \left(\frac{\mu}{3}+M\right)L^2 & MLR \\ MLR & \frac{7}{5}MR^2 \end{bmatrix} \\ B &= \begin{bmatrix} S+K+\left(\frac{\mu L}{2}+ML\right)(g+\ddot{\eta}) & -K \\ -K & K+MR(g+\ddot{\eta}) \end{bmatrix} \end{aligned}$$

and

$$v = \begin{bmatrix} - \left( \frac{\mu L}{2} + ML \right) \ddot{\xi} \\ -MR\ddot{\xi} \end{bmatrix}.$$

This equation represents two coupled nonhomogeneous Hill's equations. The uncoupling of homogeneous Hill's equations has been treated by Hsu.<sup>28</sup>

Multiplying by  $A^{-1}$ ,

$$\ddot{x} + A^{-1} Bx = A^{-1}v.$$

Define the co-ordinates  $y$  by

$$x = Cy$$

where the matrix  $C$  has for its columns the time-dependent eigenvectors of  $A^{-1}B$ , i.e.,

$$C^{-1}A^{-1}BC = D$$

where  $D$  is a diagonal matrix having the time-dependent eigenvalues of  $A^{-1}B$  for its elements.<sup>22</sup>

Then

$$C\ddot{y} + A^{-1}BCy = A^{-1}v$$

and  $\ddot{y} + C^{-1}A^{-1}BCy = C^{-1}A^{-1}v$

i.e.  $\ddot{y} + Dy = C^{-1}A^{-1}v. \dots(3)$

This last matrix equation represents two uncoupled second order nonhomogeneous ordinary differential equations with time-varying coefficients (two nonhomogeneous uncoupled Hill's equations).

If the vertical motion of the support  $\eta(t)$  is small, then the time-dependent eigenvalues of  $A^{-1}B$  may be expanded in a power series of  $\dot{\eta}(t)$  and terms of order  $\dot{\eta}^2$  may be neglected.

This gives:

$$D = D_0 + D_1 \dot{\eta}(t)$$

where  $D_0$  is a diagonal matrix with the values of  $\omega^2$  as obtained from Eqn (1) for its elements, and where  $D_1$  is also a diagonal matrix.

If it is further assumed that the support motions are sinusoidal with circular frequency  $\Omega$ , then:

$$\eta(t) = a \cos \Omega t$$

and  $\xi(t) = b \cos (\Omega t + \alpha)$

where  $a =$  vertical amplitude of the support motion (assumed to be small)

$b =$  horizontal amplitude of the support motion

$\alpha =$  phase angle between vertical and horizontal motions.

Eqn (3) then becomes two uncoupled nonhomogeneous Mathieu equations, the stability of which is well known.

For the present application, we desire the frequencies  $\Omega$  which will cause the greatest instability. The nonhomogeneity in Eqn (3) is proportional to the column vector  $v$ , i.e., is proportional to  $\dot{\xi}(t)$ . Kotowski<sup>23</sup> has discussed the nonhomogeneous Mathieu equation in which the nonhomogeneity is sinusoidal of the same frequency as the sinusoidal coefficient in the homogeneous equation. She showed that for this case, the stability diagram for the nonhomogeneous equation is identical to the stability diagram for the homogeneous equation. The unstable solutions of the nonhomogeneous equation possess greater instability than the corresponding unstable solutions of the homogeneous equation, a property which is desirable in the present application.

Thus, to find the frequencies  $\Omega$  causing the greatest instability, it is sufficient to examine the stability of the two homogeneous Mathieu equations represented by the matrix equation:

$$\ddot{y} + [D_0 - D_1 a \Omega^2 \cos \Omega t]y = 0.$$

Setting  $\tau = \Omega t$  this becomes:

$$\frac{d^2 y}{d\tau^2} + \left[ \frac{1}{\Omega^2} D_0 - D_1 a \cos \Omega t \right] y = 0.$$

For small  $a$ , the greatest instability<sup>24, 25</sup> occurs for those values of  $\Omega$  such that:

$$\frac{1}{\Omega^2} D_0 = \begin{bmatrix} 1/4 & 0 \\ 0 & 1/4 \end{bmatrix}$$

and since  $D_0$  has the square of the natural frequencies of the planar motions for its diagonal elements,

$$\Omega = 2\omega.$$

That is, as in the case of a simple pendulum with a vertically oscillating<sup>14, 26</sup> support, the maximum instability occurs when the frequency of the support motion is twice the natural frequency.

This analysis has provided, however, two frequencies  $\Omega$  causing the greatest instability (since there are two natural frequencies  $\omega$  resulting from Eqn (1)). If

$$y = \begin{bmatrix} y_1 \\ y_2 \end{bmatrix}$$

then one value of  $\Omega$  will cause  $y_1$  to be unstable while the other value of  $\Omega$  will cause  $y_2$  to be unstable. In order to choose the appropriate value of  $\Omega$ , the mode shapes must be considered.

The matrix  $C$  was defined above to have for its columns the time-dependent eigenvectors of  $A^{-1}B$ . If, as has been assumed,  $\eta(t)$  is small, then these eigenvectors are nearly equal to the eigenvectors of the undriven model, i.e., they are nearly equal to the modal vectors.<sup>27</sup> Suppose the mode shape corresponding to the in-phase planar mode is  $\varphi/\theta = c_1$  and to the out-of-phase planar mode is  $\varphi/\theta = c_2$ , respectively, then:

$$C \approx \begin{bmatrix} 1 & 1 \\ c_1 & c_2 \end{bmatrix}$$

and since  $x = Cy$

$$\theta \approx y_1 + y_2$$

$$\varphi \approx c_1 y_1 + c_2 y_2.$$

Now if  $\Omega$  is twice the natural frequency corresponding to the in-phase planar mode,  $y_1$  will be unstable while  $y_2$  will be stable. After some time  $y_1 \gg y_2$  and  $\varphi/\theta \approx c_1$ . Similarly if  $\Omega$  is twice the natural frequency corresponding to the out-of-phase mode, then:

$$\frac{\varphi}{\theta} \approx c_2.$$

### 3. Discussion

The mode for which  $[(\bar{\varphi}/\bar{\theta}) - 1] > 0$  corresponds to the in-phase planar motion<sup>27</sup> and the out-of-phase planar motion corresponds to  $[(\bar{\varphi}/\bar{\theta}) - 1] < 0$  as described by Diener *et al.*<sup>15</sup>

In each numerical evaluation of Eqn (1) for parameters representative of typical fruit samples the lower frequency was found to correspond to in-phase motion and the higher frequency resulted in out-of-phase motion (*see* Table I). In some fruit removal processes, failure should be induced between the stem and the supporting member (such as apples and citrus fruits) for appearance and for the reduction of fruit contamination. In other fruits (such as cherries) the type of processing will determine the desirability of detaching the fruit without the stem. For stems to

remain attached, the natural frequency corresponding to the smaller value of  $|(\bar{\varphi}/\theta) - 1|$  should be selected. However, if  $|(\bar{\varphi}/\theta) - 1| \approx 0$  then the entire fruit and stem move nearly as a single rigid pendulum, i.e., there is little bending of the fruit relative to the stem. In such a case, the greatest strain occurs between the stem and the limb, and a fruit excited in such a mode is most likely to be removed with its stem. In any particular case, Eqn (1) should be solved for the two natural frequencies,  $\omega_1$  and  $\omega_2$ , and then Eqn (2) should be solved for the associated planar mode shapes. Then, inspection of the mode shapes and consideration of the fruit being harvested will determine which mode is to be excited.

According to the preceding analysis, the shaking frequency should be twice the appropriate natural frequency whenever there exists a vertical component of oscillation of the supporting member.

The fruits have been assumed to be independently suspended and to be free to oscillate without contact with other bodies. Obviously, certain spur apples must then be excluded from the present discussion. The analysis has implicit, also, the assumption of collinearity of the principal axes of the stem and fruit in their equilibrium configuration, such as is not necessarily the case with lemons. The expression for the Lagrangian may be easily modified to include other equilibrium configurations by including initial displacement constants.

The flexibility of the stem is accounted for by the inclusion of torsion springs at the joints; this assumption permits a finite degree-of-freedom analysis.

The mass of the fruit stem in relation to that of the fruit is usually so small that little inaccuracy is incurred by setting  $\mu=0$ . The radius of the fruit may often be taken as the radius of a sphere of equivalent volume. For typical apple sizes, the resulting error is very small as shown in the appendix. The apple is mathematically modelled through the use of bispherical co-ordinates. In addition to the principal moments of inertia and radii of gyration, the surface area and volume which are useful in other contexts as well are calculated.

The elliptic path of the stem support is not, in general, the same as that of the shaker. However, the tree structure does oscillate with the frequency of the shaker.<sup>15</sup> Experimental investigations<sup>16, 17</sup> have shown that only a small time is required for certain tree structures to reach a steady state of vibration due to the action of the shaker. Although the magnitude of the stroke is known to be important, attention has been confined to small displacements of the stem support.

The amplitude attenuation or amplification in the transmission through the tree may be a limiting factor, especially with long willow hangers. The effect of the frequency of the vibration upon the tree structure (such as bark damage), fruit damage (to mature and immature fruit), leaf removal, the modal shapes of the limbs, and power requirements are extensively described in the literature and are not described here.

Much of the data relevant to this problem to be found in the literature deals with the (ultimate) strength beyond the elastic limit. The present analysis demonstrates a need to know the stem stiffness within the elastic limit. Table I shows some typical values for the fruit mass, fruit radius, stem mass and stem length for apples,<sup>36</sup> cherries,<sup>3</sup> and grapefruits.<sup>17</sup> The torsional spring constants are approximations only. Also, observe that fruit mass and fruit radius are not independent but must be related by the average density of the fruit.

Diener *et al.*<sup>15</sup> observed the principal modes and frequencies for various apple fruit supporting systems. Directly attached fruit exhibited pendulum mode vibrations for frequencies of 80–180 cycles/min. The tilting mode appeared for 220–340 cycles/min. The rotational mode occurred in the range of 350–450 cycles/min. The point of separation was found to be, respectively, in the abscission zone, at the fruit and in the abscission zone, and at the fruit. Thomas<sup>12</sup> reported natural frequency data for six apple varieties as follows: Stayman, 143–222 cycles/min (mean of 181.5); Rome Beauty, 130–177 cycles/min (mean 151.0); McIntosh, 166–273 (mean 204.7); Red Delicious, 143–200 (mean 166.5); Starr, 139–215, (mean 170.5); Minnesota 838, 136–184 (mean 158.8). The period of free oscillation for apples initially displaced 10 degrees was used for each of the 100 apples in each of Thomas' samples.

From Table I, the natural frequencies of apples (based on the estimated stiffness of  $S=K \leq 1.67 \times 10^{-2}$  ft lb/radian) may be expected to be between 10 and 18 radians/s (95.5–171.9 cycles/min) for the pendulum mode and between 36 and 110 radians/s (343.8–1050.4 cycles/min) for the tilting mode. The predicted pendulum frequencies substantially agree with the reported experimental data.<sup>12, 15</sup> The predicted tilting mode frequency is higher than reported.<sup>15</sup> Also, changes in the relative stiffness of the two spring constants ( $S$  very large,  $K$  very small) could effectively prevent pendulum type behaviour at the lower frequency. The analysis indicates that the shaking frequency for apples should be twice the pendulum frequency when a vertical component of excitation is present. In other words, the shaking frequency for apples should probably fall between 200 and 350 cycles/min, which is still less than the tilting mode natural frequency range predicted by this model.

An excitation with a deliberately imposed small vertical component might reduce the inadvertent stimulation of the higher natural frequency mode. In general, an increase in stem length will reduce both natural frequencies (for all dimensions checked). On the other hand, an increase in the spring constants will increase both natural frequencies. The lower frequency is much less affected by the spring constants than the higher frequency. The increase in apple mass and radius during the period 110 to 130 days after full bloom do not appreciably affect the vibratory behaviour of the fruit.

The analysis indicates that cherries may be harvested with stems attached if the shaking frequency is in the range of 250 to 325 cycles/min and harvested without stems if the shaking frequency (with a vertical component) is in the range of 1000 to 1700 cycles/min. (The tilting mode is very pronounced.) In other words, the undesirable stem-removal operation might be minimized if frequencies much higher than the currently used 1000 cycles/min were used.

The predicted natural frequencies for Marsh grapefruit are 70 to 130 cycles/min and 275 to 750 cycles/min for pendulum and tilting modes, respectively. Rumsey found that with horizontal excitation, a grapefruit with a 4 inch stem would fail with a stem attached for a frequency of 100 to 130 cycles/min and without the stem for a frequency of 300 to 400 cycles/min. The actual shaking frequency, again, should be twice the higher natural frequency range, whenever a vertical component of excitation exists.

The rotational natural frequency prediction for apples will exceed the actual value since the moment of inertia for that axis may be 11% smaller than the actual value as shown in Table II (and as derived in the Appendix).

On the other hand, the use of a sphere of equivalent volume for the other principal axis calculation will yield a positive error of only 4% for an apple with a width : height ratio of 1.25. The use of the simplified geometry is, therefore, justified.

#### 4. Conclusions

The natural frequencies and mode shapes for the vibratory harvest of freely suspended fruit may be predicted. The analysis indicates that the greatest dynamic instability of the fruit occurs at a shaking frequency of twice the natural frequency when the upper end of the stem undergoes small, planar, elliptical displacements. When fruit detachment occurs by fatigue failure of the stem, the fruit may be separated with or without the stem attached, as desired, by choosing the proper natural frequency.

On the basis of estimated stem stiffness, excellent agreement with experimental data was found for the three fruits for which documentation was available in the literature. The calculations indicate that lower frequencies for apples and higher frequencies for cherries (harvested without stems) than are currently being used should be experimentally examined. The stem stiffness ( $S$  and  $K$ ) should be studied for seasonal, genetic, and chemically induced changes and for its possible value as an indicator of "readiness for harvest". Also, a statistical study of the usual biological variability of the parameters used in the model must be made before reliable recommendations can be made.



Finally, a mathematical model of the apple (using bispherical co-ordinates) was developed and was used to demonstrate the validity and usefulness of treating the fruit as a sphere of equivalent volume in the calculation of the moments of inertia.

A consideration of factors not examined in this paper could alter the choice of shaking frequency. Specifically, the time to remove all the fruit from a tree may not necessarily be minimized with the specified frequency and small amplitude of vibration. Also, note that we have not considered detachment due to an impulsive tensile force.

### Acknowledgements

The computational assistance of Messrs. James McDaniels and Larry VanVleet is gratefully acknowledged.

### REFERENCES

- <sup>1</sup> Markwardt, E. D.; Guest, R. W.; Cain, J. C.; LaBelle, R. L. *Mechanical cherry harvesting*. Trans. ASAE, 1964, 7 (1), 70–74, 82
- <sup>2</sup> Barnes, K. K. *Detachment characteristics of lemons*. ASAE Paper 68–121. ASAE, St. Joseph, Michigan
- <sup>3</sup> Tennes, B. R.; Levin, J. H.; Stout, B. A. *Sweet cherry properties useful for designing harvesting and handling equipment*. ASAE Paper 68–348, ASAE, St. Joseph, Michigan
- <sup>4</sup> Graf v. Hardenberg, D. W. *Die Mechanisierung der Ernte von Stein- und Strauchbeerenobst*. (English translation by Dipl. Ing. Werner Hoefflinger, Dept. Agr. Engr., Cornell University.) KTL-Berichte über Landtechnik 115, 1967
- <sup>5</sup> Coppock, G. E.; Hedden, S. L.; Lenker, D. H. *Biophysical properties of citrus fruit related to mechanical harvesting*. ASAE Paper 68–117, ASAE, St. Joseph, Michigan
- <sup>6</sup> Moore, M. J. *et al.* *Principles of harvesting hanging fruits*. Annual Report of Cooperative Regional Project No. 564, USDA, January 1 to December 31, 1964, New Brunswick, New Jersey
- <sup>7</sup> Lamouria, L. H.; Brewer, H. L. *Determining selected bioengineering properties of olives*. Trans ASAE, 1965, 8 (2) 271
- <sup>8</sup> Wang, Jaw-Kai. *Mechanical coffee harvesting*. Trans. ASAE, 1965, 8 (3) 400
- <sup>9</sup> Wang, Jaw-Kai; Shellenberger, F. A. *Effects of cumulative damage to stress cycles on selective harvesting of coffee*. Trans. ASAE, 1967, 10 (2) 252
- <sup>10</sup> Studer, H. E. *Mechanical harvesting of Concord grapes*. M.Sc. Thesis, 1962, Mann Library, Cornell University.
- <sup>11</sup> Diener, R. G.; Levin, J. H.; Whittenberger, R. T. *Frequency and stroke studies for shaking apples*. ASAE Paper 68–662, ASAE, St. Joseph, Michigan
- <sup>12</sup> Thomas, R. L. *The importance of the frequency of applied forces in pneumatic fruit harvesting*. ASAE Paper 63–642B, ASAE, St. Joseph, Michigan
- <sup>13</sup> Singley, M. E.; Moore, M. J.; Childers, N. F. *Principles of harvesting hanging fruits*. Annual Reports of Project 564, USDA, 1961–62, New Brunswick, New Jersey
- <sup>14</sup> Shepardson, E. S.; Studer, H. E.; Shaulis, N. J.; Moyer, J. C. *Mechanical grape harvesting*, J. Am. Soc. Agric. Engng, 1962 43 (2) 66
- <sup>15</sup> Diener, R. G.; Mohsenin, N. N.; Jenks, B. L. *Vibration characteristics of trellis-trained apple trees with reference to fruit detachment*. Trans. ASAE, 1965, 20
- <sup>16</sup> Studer, H. E. *Motion of pendular fruit systems during vertical vibration*. ASAE Paper 66–635, 1966, ASAE, St. Joseph, Michigan
- <sup>17</sup> Rumsey, J. W. *Response of citrus fruit-stem system to fruit removing actions*. M.S. Thesis, January, 1967, University of Arizona, Tucson
- <sup>18</sup> Abu-Gheida, O. M.; Stout, B. A.; Ries, S. K. *Pneumatic tree-fruit harvesting utilizing a pulsing air stream*. J. Agr. Engr., 1962, 43 (8) 458
- <sup>19</sup> Flügge, W. (ed.). *Handbook of engineering mechanics*. McGraw-Hill Book Company, 1962, New York, pp. 61–66, 55–6
- <sup>20</sup> Baker, W. E. *Vibration frequencies for uniform beams with central masses*. J. Applied Mechanics, 1964, 86 (3) 335
- <sup>21</sup> Symon, K. *Mechanics*, 2nd ed. Addison-Wesley Publishing Company, Reading, Mass., 1960, p. 107

- <sup>22</sup> Hildebrand, F. B. *Methods of applied mathematics*, 2nd ed. Prentice-Hall, Englewood Cliffs, New Jersey, 1965, p. 37
- <sup>23</sup> Kotowski, G. *Lösungen der inhomogenen Mathieschen Differentialgleichung mit periodischer Störfunktion beliebiger Frequenz*. Z. angew Math. Mech Bd., 1943 23 (4) 213
- <sup>24</sup> Stoker, J. J. *Nonlinear vibrations*. Interscience. New York, 1950
- <sup>25</sup> McLachlan, N. W. *Theory and application of Mathieu functions*, Dover Pub., New York, 1964
- <sup>26</sup> Lord Raleigh. *Theory of Sound*. Dover Pub., New York, 1945, p. 82
- <sup>27</sup> Tong, K. N. *Theory of mechanical vibrations*, John Wiley, New York, 1960, p. 177
- <sup>28</sup> Hsu, C. S. *On a restricted class of coupled Hill's equations and some applications*. Journal of Applied Mechanics, 1961, 28 (4) Series E, 551
- <sup>29</sup> Moon, P.; Spencer, D. E. *Field theory for engineers*. Van Nostrand, 1961, Ch. 3, 13
- <sup>30</sup> Moon, P.; Spencer, D. E. *Field theory handbook*. Springer-Verlag, Berlin, 1961, p. 110
- <sup>31</sup> Morse, P. M.; Feshbach, H. *Methods of theoretical physics*. McGraw-Hill, New York, 1953 Part I, p. 665 ff.
- <sup>32</sup> Gradshteyn, I. S.; Ryzhik, I. M. *Tables of integrals, series and products*. Academic Press, New York, 1965, pp. 107-108
- <sup>33</sup> Megilley, B. W.; Rasmussen, H. P.; Dewey, D. H. *Fruit characteristics affecting apple orientation in water*, Michigan Agr. Experiment Station Quarterly Bulletin, 1968, 50 (4) 527
- <sup>34</sup> Turrell, F. M.; Vanselow, A. P. *Tables of coefficients for estimating oblate and prolate spheroidal surfaces and volumes from spherical surfaces and volumes. For finding fruit surfaces and volumes*. Proceedings American Society for Horticultural Science, 1946, 48 (3) 326
- <sup>35</sup> Moustafa, S.; Stout, B. A. *A mathematical model for the apple fruit*, Michigan Agr. Experiment Station Quarterly Bulletin, 49 (4) 450
- <sup>36</sup> Westwood, M. N. *Seasonal changes in specific gravity and shape of apple, pear and peach fruits*. Proceedings American Society for Horticultural Science, 1962, 80 (0) 90
- <sup>37</sup> Vis, E.; Wolf, D.; Stout, B. A.; Dewey, D. H. *Physical properties of apple fruit pertaining to orientation*. ASAE Paper 68-333, 1968, ASAE, St. Joseph, Michigan

### Appendix

The assumption of spherical fruit will be examined. Using bispherical co-ordinates<sup>29, 30, 31</sup> moments of inertia for a more general and more realistic shape may be calculated. Taking the z-axis as the axis of rotation, the transformation between the bispherical and Cartesian co-ordinates is:

$$x = \frac{a \sin \theta \cos \psi}{\cosh \eta - \cos \theta} \quad \dots(A1)$$

$$y = \frac{a \sin \theta \sin \psi}{\cosh \eta - \cos \theta} \quad \dots(A2)$$

$$z = \frac{a \sinh \eta}{\cosh \eta - \cos \theta} \quad \dots(A3)$$

where

$$-\infty < \eta < \infty$$

$$0 \leq \theta \leq \pi$$

$$0 \leq \psi < 2\pi.$$

The surfaces<sup>30</sup> of constant  $\eta$  are spheres with the sphere for  $\eta > 0$  above the x-y plane.

$$x^2 + y^2 + (z - a \coth \eta)^2 = \frac{a^2}{\sinh^2 \eta} \quad \dots(A4)$$

The surfaces of constant  $\theta$  are lemon-(spindle), orange-(sphere), and apple-shaped (with dimples) and are described by:

$$x^2 + y^2 + z^2 - 2a(x^2 + y^2)^{\frac{1}{2}} \cot \theta = a^2 \quad \dots(A5)$$

TABLE I  
Natural frequencies and mode shapes for various fruits based on estimated parameters\*

	M, slug	R, ft	$\mu$ , slug	L, ft	S, ft lbf radian <sup>-1</sup>	K, ft lbf radian <sup>-1</sup>	$\omega_1$ , radian/sec	$\omega_2$ , radian/sec	$\left[\frac{\phi}{\theta}(\omega_1) - 1\right]$	$\left[\frac{\phi}{\theta}(\omega_2) - 1\right]$
Golden Delicious	(-3) 7.13	(-1) 1.03	(-6) 6.25	(-2) 6.96 (-1) 1.67	0 0 (-2) 1.67	<b>Apples†</b> 0 0 (-2) 1.67 0	12.7 10.6 11.8 12.3	47.3 36.7 56.0 46.6	+0.26 +0.17 +0.31 +0.27	-1.54 -2.39 -2.38 -1.48
	(-3) 9.94	(-1) 1.14	(-6) 6.25	(-2) 6.96	0	0	11.7	41.2	+0.22	-1.79
Rome Beauty	(-3) 8.43	(-1) 1.07	(-6) 6.25	(-1) 1.04	0 (-2) 1.67	0 (-2) 1.67	13.0	65.3	+0.42	-1.78
	(-2) 1.23	(-1) 1.22	(-6) 6.25	(-1) 1.04	0 (-2) 1.67	0 (-2) 1.67	11.2 12.0	40.2 56.9	+0.24 +0.41	-1.69 -1.68
Jonathan	(-3) 6.31	(-2) 9.94	(-6) 6.25	(-2) 6.96	0 (-2) 1.67	0 (-2) 1.67	12.9 15.0	47.6 92.8	+0.26 +0.53	-1.56 -1.55
				(-2) 4.17	0	0	13.7	57.7	+0.30	-1.32
				(-2) 8.33	0	0	12.5	44.8	+0.24	-1.68
				(-1) 1.25	0	0	11.5	39.7	+0.20	-2.05
	(-3) 8.77	(-1) 1.11	(-6) 6.25	(-2) 6.96	0 (-3) 1.67 (-2) 1.67 (-1) 1.67	0 (-3) 1.67 (-2) 1.67 (-1) 1.67	12.4 12.5 13.8 22.5	46.8 51.2 80.8 213.4	+0.27 +0.33 +0.52 +0.65	-1.49 -1.49 -1.49 -1.49
Delicious	(-3) 9.05	(-1) 1.09	(-6) 6.25	(-2) 6.96	0 (-2) 1.67 0 (-2) 1.67 (-1) 1.67	0 (-2) 1.67 (-2) 1.67 0 0	12.5 13.8 12.5 13.3 14.3	46.9 80.2 71.7 59.3 124.4	+0.27 +0.51 +0.10 +1.40 +11.75	-1.50 -1.50 -1.51 -1.48 -1.46
				(-1) 1.25	(-1) 1.67	(-1) 1.67	19.3	142.0	+0.49	-1.94
	(-2) 1.21	(-1) 1.21	(-6) 6.25	(-2) 6.96	0 (-2) 1.67	0 (-2) 1.67	12.0 12.9	46.3 71.9	+0.28 +0.50	-1.45 -1.45
Yellow Newton	(-3) 7.33	(-1) 1.01	(-6) 6.25	(-2) 6.96	0 (-2) 1.67	0 (-2) 1.67	12.8 14.6	47.5 87.6	+0.26 +0.52	-1.55 -1.54
	(-2) 1.00	(-1) 1.12	(-6) 6.25	(-2) 6.96	0 (-2) 1.67	0 (-2) 1.67	12.3 13.6	46.7 77.3	+0.27 +0.51	-1.49 -1.48
Winesap	(-3) 3.56	(-2) 7.93	(-6) 6.25	(-2) 8.33	0 (-2) 1.67	0 (-2) 1.67	13.4 17.5	46.8 110.4	+0.22 +0.48	-1.87 -1.85
	(-3) 5.21	(-2) 9.00	(-6) 6.25	(-2) 8.33	0 (-2) 1.67	0 (-2) 1.67	12.9 15.5	45.6 91.4	+0.23 +0.48	-1.75 -1.74
Windsor	(-4) 3.64	(-2) 3.52	(-6) 6.73	(-1) 1.21	<b>Cherries‡</b> 0 (-5) 5.00 (-4) 5.00	0 0 (-5) 5.00 (-4) 5.00	14.2 14.4 16.0	54.5 58.8 88.7	+0.10 +0.12 +0.19	-4.15 -4.14 -4.13
Schmidt	(-4) 4.42	(-2) 3.68	(-6) 6.89	(-1) 1.25	0 (-4) 5.00	0 (-4) 5.00	14.0 15.3	53.5 81.1	+0.10 +0.18	-4.10 -4.09
Napoleon	(-4) 4.21	(-2) 3.66	(-6) 6.29	(-1) 1.06	0 (-4) 5.00	0 (-4) 5.00	14.8 16.5	54.8 85.9	+0.12 +0.21	-3.61 -3.59
Marsh	(-2) 2.05	(-1) 1.25	(-5) 5.06	(-1) 1.67	<b>Grapefruit§</b> 0 (-2) 1.67 (-1) 1.67	0 0 (-2) 1.67 (-1) 1.67	10.1 10.5 13.3	34.9 41.7 80.2	+0.19 +0.27 +0.42	-2.12 -2.12 -2.11
	(-2) 2.05	(-1) 1.25	(-4) 1.01	(-1) 3.33	0 (-2) 1.67 (-1) 1.67	0 (-2) 1.67 (-1) 1.67	8.3 8.5 10.2	30.2 34.4 60.5	+0.12 +0.16 +0.25	-3.38 -3.38 -3.37
	(-2) 2.05	(-1) 1.25	(-4) 1.52	(-1) 5.00	0 (-2) 1.67 (-1) 1.67	0 (-2) 1.67 (-1) 1.67	7.1 7.3 8.4	28.5 32.1 54.4	+0.09 +0.11 +0.18	-4.69 -4.69 -4.68

\*Floating decimal notation, e.g. (-3) 7.13 =  $7.13 \times 10^{-3}$

†M and R data from Westwood<sup>26</sup>

‡M, R, and L data from Tennes *et al.*<sup>3</sup>

§M, R,  $\mu$  and L data from Rumsey<sup>17</sup>

for  $\pi > \theta \geq \frac{\pi}{2}$ ,  $\theta = \frac{\pi}{2}$ , and  $\frac{\pi}{2} > \theta \geq 0$

respectively. The constant  $a$  is the focal length and is the distance from the origin to the intersection of the  $\theta$  surface with the  $z$ -axis. The longitudinal cross sections for selected  $\theta$  values are shown in Fig. 3. In each case, the circular arcs have radii of  $a (\csc \theta)$  and centres at  $x_c = a (\cot \theta)$ .

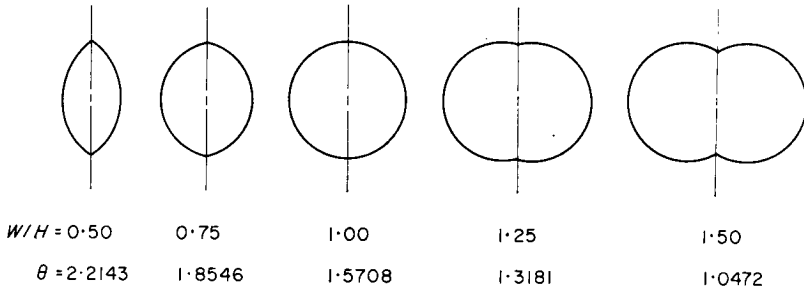


Fig. 3. Bispherical shapes (with constant height) for width: height ratios (left to right) of 0.50, 0.75, 1.00, 1.25, 1.50

Note that  $x_c > 0$  for  $\theta < \frac{\pi}{2}$  and  $x_c < 0$  for  $\theta > \frac{\pi}{2}$ . Surfaces of constant  $\psi$  are half-planes which emanate from the  $z$ -axis.

$$\tan \psi = \frac{y}{x} \tag{A6}$$

This co-ordinate system has sufficient generality to include the shapes of most of the mechanically harvested fruits. The spindle shapes are similar to prolate spheroids. As the width : height ratio  $W/H$  increases, the spindle shape becomes spherical, and then apple-shaped. For  $W/H = 2$ , a doughnut shape (a toroid), without a hole, results. The width-to-height ratio can be shown to determine the value of  $\theta$ .

$$\frac{W}{H} = \begin{cases} 1 + \cos \theta, & 0 < \theta \leq \frac{\pi}{2}, \text{ apple shape} \\ (1 + \cos \theta) / \sin \theta, & \frac{\pi}{2} \leq \theta < \pi, \text{ lemon shape} \end{cases} \tag{A7}$$

The functional dependence of  $\theta$  upon the width : height ratio (Eqn (7)) is shown graphically in Fig. 3.

The over-all height  $H$  is:

$$H = \begin{cases} (2a) / \sin \theta, & 0 < \theta \leq \frac{\pi}{2} \\ 2a, & \frac{\pi}{2} \leq \theta < \pi \end{cases} \tag{A8}$$

Eqns (7) and (8) determine the value of  $a$ . The total width is:

$$W = 2a(1 + \cos \theta) / \sin \theta, \quad 0 < \theta < \pi. \tag{A9}$$

Since the bispherical co-ordinate system is orthogonal, the expressions for the surface area  $A$ , volume  $V$ , and principal moments of inertia  $I_z, I_x$  may be easily formed.

$$A = 2a^2 \int_{\eta=0}^{\infty} \int_{\psi=0}^{2\pi} \frac{\sin \theta \, d\psi \, d\eta}{(\cosh \eta - \cos \theta)^2} \tag{A10}$$

For  $\theta \neq 0, \pi$  this equation becomes<sup>32</sup>

$$A = 4\pi(a/\sin \theta)^2 [\sin \theta + (\pi - \theta) \cos \theta]. \quad \dots(A11)$$

This equation may be normalized by dividing by the surface area of a sphere having the same height as the body in question. The spindle shapes will be enclosed by such a sphere; the apple shapes will not be completely enclosed. From Eqns (11) and (8).

$$\frac{A}{4\pi(H/2)^2} = \begin{cases} [\sin \theta + (\pi - \theta) \cos \theta], & 0 < \theta \leq \frac{\pi}{2} \\ [\sin \theta + (\pi - \theta) \cos \theta] / \sin^2 \theta, & \frac{\pi}{2} \leq \theta < \pi \end{cases} \quad \dots(A12)$$

$$\equiv \sigma$$

A similar normalization has been used by Turrell and Vanselow<sup>34</sup> for prolate and oblate spheroids. An actual surface area may be obtained by multiplying the  $\sigma$  value from Fig. 4 (or Eqn (12)) by the surface area of a sphere having the same height.

$$A = \sigma A_{\text{sphere}} \quad \dots(A13)$$

The volume  $V$  is

$$V = 2a^3 \int_{\eta=0}^{\infty} \int_{\theta=0}^{\pi} \int_{\psi=0}^{2\pi} \frac{\sin \theta \, d\psi \, d\theta \, d\eta}{(\cosh \eta - \cos \theta)^3} \quad \dots(A14)$$

The volume may be expressed<sup>32</sup> as

$$V = [2\pi/3] [a/\sin \theta]^3 [3 \sin \theta + 3(\pi - \theta) \cos \theta - \sin^3 \theta], \theta \neq 0, \pi. \quad \dots(A15)$$

This equation may also be normalized by dividing the equation by the volume of a sphere of the same height.

$$\frac{V}{(4/3)\pi(H/2)^3} = \begin{cases} (1/2) [3 \sin \theta + 3(\pi - \theta) \cos \theta - \sin^3 \theta], & 0 < \theta \leq \frac{\pi}{2} \\ (1/2) [3 \sin \theta + 3(\pi - \theta) \cos \theta - \sin^3 \theta] / [\sin^3 \theta], & \frac{\pi}{2} \leq \theta < \pi \end{cases} \quad \dots(A16)$$

$$\equiv v.$$

Therefore,

$$V = v V_{\text{sphere}} \quad \dots(A17)$$

The  $\sigma$  and  $v$  curves are shown in Fig. 4. Both curves monotonically increase with  $W/H$  and are equal to unity for  $W/H=1$ . A tabulation of  $\theta, \sigma, v$  and their biological significance will be presented elsewhere.

The moment of inertia about the axis of symmetry  $I_z$  is

$$I_z = \int_v r^2 \, dm$$

$$I_z = \rho a^5 \int_{\eta=-\infty}^{\infty} \int_{\theta=0}^{\pi} \int_{\psi=0}^{2\pi} \frac{\sin^3 \theta \, d\psi \, d\theta \, d\eta}{[\cosh \eta - \cos \theta]^5} \quad \dots(A18)$$

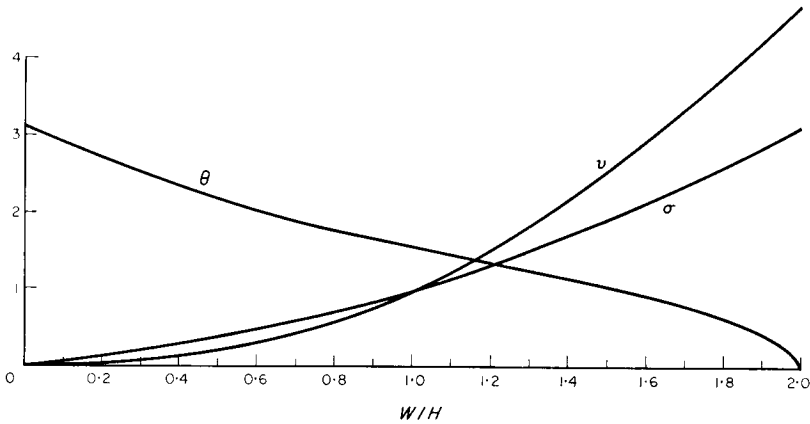


Fig. 4. The width: height ratio determines the shape variable  $\theta$ , the normalized surface area  $\sigma$ , and the normalized volume  $\nu$

where the mass density  $\rho$  is assumed to be constant. The actual apple density is known to vary slightly.<sup>33, 36</sup> (The core is slightly more dense than the cortex and the centre of gravity is slightly nearer the stem end.<sup>37</sup>) Integration<sup>32</sup> of Eqn (18) yields

$$I_z = (\pi\rho/2) (a/\sin \theta)^5 \{ 7 \sin \theta - (19/3) \sin^3 \theta + 7 \cos \theta [1 - (4/7) \sin^2 \theta] [\pi - \theta] + (2/5) \sin^5 \theta \}, \theta \neq 0, \pi \quad \dots(A19)$$

when normalized, Eqn (19) becomes:

$$\frac{I_z}{(1/60) \rho \pi H^5} = \begin{cases} (3/32) \{ 7 \sin \theta - (19/3) \sin^3 \theta + 7 \cos \theta [1 - (4/7) (\sin^2 \theta)] \cdot (\pi - \theta) + (2/5) \sin^5 \theta \}, & 0 < \theta \leq \frac{\pi}{2} \\ (3/32) \{ 7 \sin \theta - (19/3) \sin^3 \theta + 7 \cos \theta [1 - (4/7) (\sin^2 \theta)] \cdot (\pi - \theta) + (2/5) \sin^5 \theta \} / [\sin^5 \theta], & \frac{\pi}{2} \leq \theta < \pi \end{cases} \quad \dots(A20)$$

The other principal moment of inertia is:

$$I_x = 2\rho a^5 \int_{\eta=0}^{\infty} \int_{\theta=0}^{\pi} \int_{\psi=0}^{2\pi} \frac{[\sin^3 \theta \sin^2 \psi + \sinh^2 \eta \sin \theta] d\psi d\theta d\eta}{[\cosh \eta - \cos \theta]^5} \quad \dots(A21)$$

$$I_x = I_y = \pi\rho(a/\sin \theta)^5 [(1/30) \sin^5 \theta - (19/12) \sin^3 \theta - (\pi - \theta) \cos \theta \sin^2 \theta + (1/12) (25 + 2 \cos^2 \theta) \sin \theta + (9/4) (\pi - \theta) \cos \theta], \quad \theta \neq 0, \pi \quad \dots(A22)$$

When normalized by dividing the moment of inertia of a sphere of the same density and same height, two dimensionless expressions are obtained. The graphs of the normalized moments of inertia are shown in Fig. 5. The two curves do not differ greatly in the region for  $W/H < 1.25$ . The two curves intersect at  $W/H = 1.0$  and at  $W/H \approx 0.8$ ; this is due to the  $\sin^5 \theta$  divisor in the expression when  $W/H < 1$ . Table II shows that the moments of inertia may be computed for an apple on the basis of a sphere of equivalent mass.

The radius of gyration is defined by

$$I = mk^2$$

TABLE II  
 Comparison of moments of inertia for bispherical apple and for equivalent volume sphere

W/H	H, ft	Vol, ft <sup>3</sup>	[R <sub>es</sub> ] <sup>*</sup> , ft	[I <sub>es</sub> /ρ] <sup>*</sup> , ft	[U <sub>z</sub> /ρ] <sup>*</sup> , ft <sup>5</sup>	[I <sub>x</sub> /ρ], ft <sup>5</sup>	% error, z-axis	% error x-axis
1.15	1.7697 × 10 <sup>-1</sup>	4.0206 × 10 <sup>-3</sup>	9.8643 × 10 <sup>-3</sup>	1.5649 × 10 <sup>-5</sup>	1.6834 × 10 <sup>-5</sup>	1.5223 × 10 <sup>-5</sup>	-7.04	+2.80
1.25	1.6273 × 10 <sup>-1</sup>	3.7956 × 10 <sup>-3</sup>	9.6771 × 10 <sup>-3</sup>	1.4219 × 10 <sup>-5</sup>	1.5968 × 10 <sup>-5</sup>	1.3631 × 10 <sup>-5</sup>	-10.95	+4.32

\* <sub>es</sub> denotes sphere of equivalent volume.

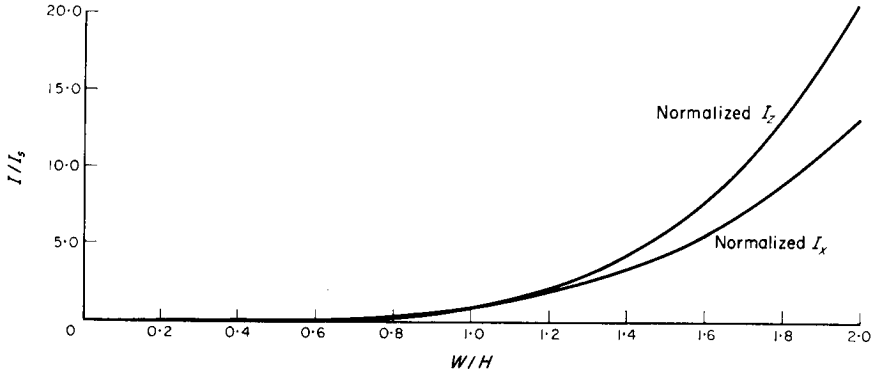


Fig. 5. The normalized principal moments of inertia are determined by the width: height ratio

and is shown for the two principal axes in Fig. 6 (normalized by division by the height  $H$ ). The  $k_z$  value is nearly linearly related to  $W/H$  and  $k_x$ , which is more complex as expected, intersects  $k_z$  at 0,1 and one intermediate point.

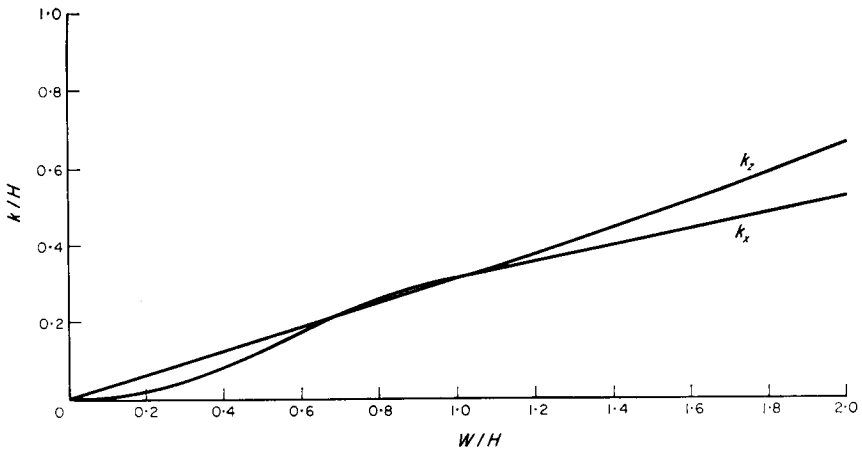


Fig. 6. The normalized radii of gyration for each principal axis is a function of  $W/H$